THE JOURNAL OF PHYSICAL CHEMISTRY C

Article

Cite This: J. Phys. Chem. C 2017, 121, 23609-23617

pubs.acs.org/JPCC

Electronic Nature of New Ir(III) Complexes: Linear Spectroscopic and Nonlinear Optical Properties

Peng Zhao,[†] Salimeh Tofighi,[†] Ryan M. O'Donnell,[‡] Jianmin Shi,[‡] Peter Y. Zavalij,[§] Mykhailo V. Bondar,*[,†,∥] David J. Hagan,[†] and Eric W. Van Stryland*[,†]

[†]CREOL, College of Optics and Photonics, University of Central Florida, Orlando, Florida 32816, United States

[‡]US Army Research Laboratory, Adelphi, Maryland 20783, United States

[§]Department of Chemistry and Biochemistry, University of Maryland, College Park, Maryland 20742, United States

[∥]Institute of Physics NASU, Prospect Nauki, 46, Kiev-28 03028, Ukraine

Supporting Information

ABSTRACT: Comprehensive investigations of the linear and nonlinear optical properties of new Ir(III) complexes [Ir(pbt)$_2$(dbm)] (**1**), [Ir(pbt)$_2$(dmac)] (**2**), and [Ir(pbt)$_2$(minc)] (**3**) (pbt = 2-phenylbenzothiazole; dbm = dibenzoyl methane; dmac = (1E,4Z,6E)-1,7-bis(4-(dimethylamino)phenyl)-5-hydroxyhepta-1,4,6-trien-3-one; minc = (1E,4Z,6E)-5-hydroxy-1,7-bis(1-methyl-1H-indol-3-yl)hepta-1,4,6-trien-3-one) are reported, including photostability, two-photon absorption, and femtosecond transient absorption spectroscopy. The steady-state and time-resolved spectral properties of **1**−**3** revealed the electronic nature of the absorption bands, and photoluminescence emission of **2** and **3** shows both fluorescence and phosphorescence processes occurring simultaneously in liquid solution at room temperature. This unusual behavior of **2** and **3** can be explained by a dual-minimum potential surface of the excited electronic state resulting in two independent fluorescence and phosphorescence emission channels. The degenerate 2PA spectra of **1**−**3** were obtained by open aperture Z-scans with a femtosecond laser, and maxima values of 2PA cross sections up to ∼350 GM were observed. Ultrafast relaxation processes of **1**−**3** were investigated by femtosecond transient absorption, and the characteristic times for triplet formation were determined to be <500 fs for **1** and ∼2 ps for **2** and **3** in a nonpolar medium.

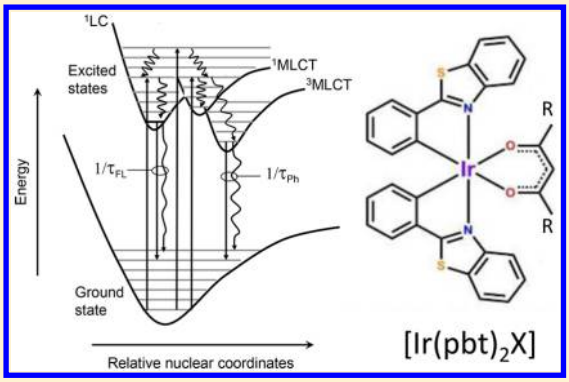

INTRODUCTION

The synthesis and characterization of new iridium complexes having a broad variety of specific linear photophysical and nonlinear optical properties[1−5] are of significance for multiple practical applications including organic optoelectronics,[6,7] bioimaging,[8,9] time-resolved luminescence sensing,[10] nonlinear optics,[11] singlet oxygen generation,[12] etc. Typically, iridium complexes bearing various ligands exhibit a variety of spectral properties due to strong spin−orbit coupling related to the heavy Ir atom[6,13] and significant metal−ligand electronic interactions.[2,14,15] Up to now, Ir(III) complexes remain the most efficient room-temperature phosphorescence emitters,[16,17] with relatively short lifetimes of the lowest excited triplet electronic states (∼1−10 μs)[15,18] and facile color tunability.[19,20] The effect of color tuning can be realized by choosing the appropriate ligand system[21,22] and/or specific protonating processes in the ligand structure.[19,23] The nature of excited-state absorption (ESA) and fast relaxation processes in the excited states have been investigated for various types of metal−ligand structures,[24−27] including polymer-based tris(2-phenylpyridine)iridium complexes,[28] iridium−silicon bonded complexes,[29] bis(1,5-cyclooctadiene)bis(μ-pyrazolyl)diiridium-(I),[30] cationic Ir(III)$^+$ complexes,[31−33] etc. It is interesting to mention that the characteristic times of singlet → triplet (S → T) transitions in Ir(III) complexes can be in the range of ∼100 fs,[3,26] and high quantum yields of S → T conversion can be observed at room temperature,[3,18,34] which creates promising applications in OLEDs[19,35] and in a number of nonlinear optical areas.[5,36] The specific metal-to-ligand electronic interactions can also be used to increase two-photon absorption (2PA) cross sections of ligands[11] and improve efficiency of their nonlinear optical processes.[37] The photochemical stability of iridium complexes is scarcely addressed in the scientific literature and was mainly investigated by relative methods[38−40] where photoinduced temporal changes in the absorption or photoluminescence intensity were analyzed without determination of the quantitative molecular parameters, such as photodecomposition quantum yield.[41]

Here we present comprehensive photophysical and nonlinear optical investigations of new Ir(III) complexes [Ir(III)-

Received: June 26, 2017
Revised: September 21, 2017
Published: September 29, 2017

DOI: 10.1021/acs.jpcc.7b06254
J. Phys. Chem. C 2017, 121, 23609−23617

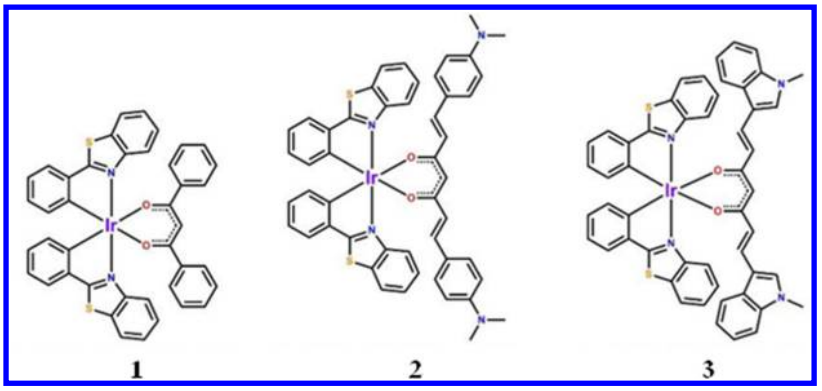

Figure 1. Chemical structures of Ir(III) complexes **1**−**3**.

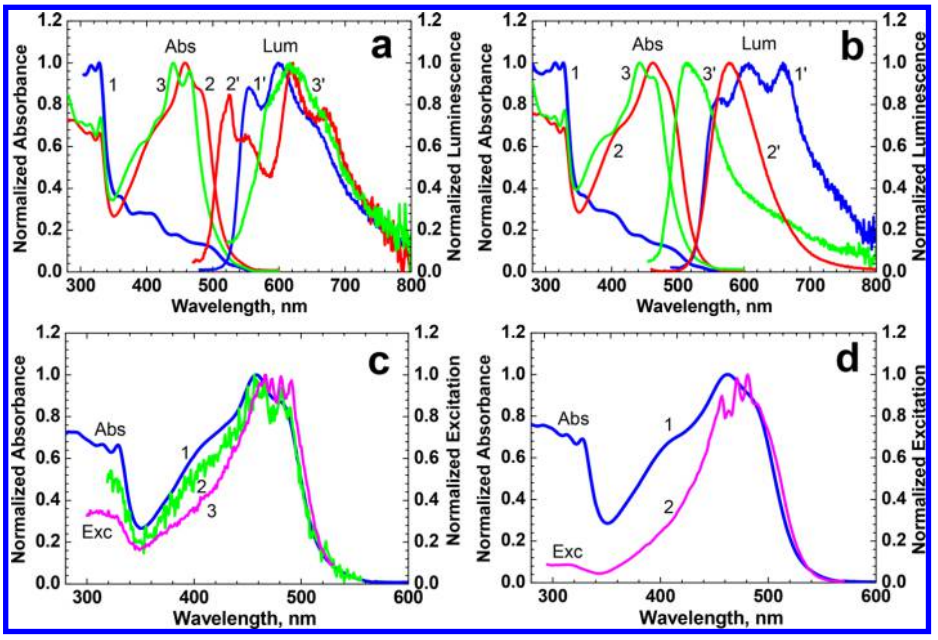

Figure 2. (a) Normalized steady-state 1PA (1−3) and PL (1′−3′) spectra of **1** (1, 1′), **2** (2, 2′), and **3** (3, 3′) in TOL. (b) Same as in panel (a) in DCM. (c) Normalized excitation (2, 3) and 1PA (1) spectra of **2** in TOL with λ_{obs} = 620 nm (2) and 550 nm (3). (d) Normalized excitation (2) and 1PA (1) spectra of **2** in DCM with λ_{obs} = 590 nm.

$(pbt)_2(dbm)]$ (**1**), $[Ir(III)(pbt)_2(dmac)]$ (**2**), and $[Ir(III)(pbt)_2(minc)]$ (**3**) in solvents of different polarity at room temperature. The main linear spectroscopic, photochemical, and nonlinear optical parameters are obtained, including excitation anisotropy spectra, photodecomposition quantum yields, characteristic time constants of fast relaxation processes in the excited states, ESA and 2PA spectra, etc. The nature of the excited-state potential surfaces of these Ir(III) complexes is revealed. The results indicate potential of these new compounds for applications in several practical areas, including organic photovoltaics, nonlinear optics, photodynamic therapy, different sensing techniques, etc.

EXPERIMENTAL SECTION

Synthesis of Ir(III) Complexes. Compounds **1**−**3** (Figure 1) were synthesized in good yields ranging from 50 to 80% via cleavage of the $[IrIII(pbt)_2Cl]_2^0$ dimer starting material and subsequent coordination of the corresponding anionic ancillary ligand in dichloromethane using modified literature procedures.[42,43] The individual β-diketonate ligands were chosen to perturb the steric and electronic environment near the iridium center and, in the case of the curcuminoid derivative compounds **2** and **3**, to enhance absorption in the visible spectrum. A detailed description of the synthesis along with ^{1}H NMR characterization and X-ray crystallographic structure determination are provided in the Supporting Information.

Linear Photophysical and Photochemical Characterization of 1−3. Linear spectral measurements were performed at room temperature in spectroscopic grade toluene (TOL), dichloromethane (DCM), butyronitrile (BTN), and acetonitrile (ACN). All solvents were purchased from commercial suppliers and used without further purification. The steady-state linear one-photon absorption (1PA) spectra of **1**−**3** were measured using a Varian CARY-500 spectrophotometer and 10 mm path length quartz cuvettes with solute concentrations $C \sim 10^{-4}$−10^{-5} M. The steady-state photoluminescence (PL), excitation, and excitation anisotropy spectra, along with the values of emission lifetimes, were obtained in dilute solutions ($C \sim 10^{-6}$ M) using spectrofluorimeter FLS980 (Edinburgh Instruments Ltd.) and spectrofluorometric quartz cuvettes with 10 mm path length. All PL spectra were corrected for spectral responsivity of the detection system. The excitation anisotropy spectra of **1**−**3** were measured at room temperature in viscous silicon oil (SiO) using the L-format configuration.[44] It should

DOI: 10.1021/acs.jpcc.7b06254
J. Phys. Chem. C 2017, 121, 23609−23617

be mentioned that the viscosity of SiO at room temperature is sufficiently high to prevent rotational depolarization effects in the case of relatively fast fluorescence emission (fluorescence lifetime $\tau_{fl} \sim 1$ ns). In this case, the molecular rotational correlation time, $\theta \gg \tau_{fl}$, so that the excitation anisotropy, $r(\lambda) = r_0(\lambda)/(1 + \tau_{fl}/\theta)$, is close to its fundamental value $r_0(\lambda)$.[44] The values of PL quantum yields, Φ_{PL}, of **1**−**3** were determined by the relative methodology of ref 44 with 9,10-diphenylanthracene in cyclohexane as a standard. The level of photochemical stability was estimated quantitatively by determining the photodecomposition quantum yields, Φ_{ph},[45,46] for **1**−**3** in all employed solvents. Corresponding values of Φ_{ph} were obtained by the absorption methodology of ref 41 using a continuous wave diode laser of excitation wavelength $\lambda_{ex} \approx 405$ nm and beam irradiance ≈ 300 mW/cm^2.

2PA Cross Sections and Femtosecond Pump−Probe Transient Absorption Measurements. The nonlinear optical properties of **1**−**3** were investigated with a femtosecond laser system. A commercial Ti:sapphire chirped-pulse-amplified Legend Duo+ (Coherent, Inc.) producing a pulsed laser beam with 1 kHz repetition rate (output wavelength 800 nm, pulse energy, $E_P \approx 12$ mJ, pulse duration, $\tau_P \approx 40$ fs) was split in two parts for Z-scan[47] and pump−probe[45,48] experimental setups. The first beam pumped an optical parametric amplifier (OPA) HE-TOPAS (Light Conversion, Inc.) with a tuning range of 1100−2600 nm and output pulse energy up to ≈2 mJ. The OPA output was filtered by multiple spike filters (fwhm ≈10 nm; output pulse duration; $\tau_P \approx 100$ fs, $E_P \leq 40$ μJ) and used for 2PA cross section measurements by the Z-scan technique over a broad spectral range. The second beam was also split in two parts for transient absorption pump−probe measurements. The first part was doubled by a 1 mm thick BBO crystal and used as a pump beam (pump wavelength, $\lambda_{pu} = 400$ nm). The second part was focused in a 1 cm path length quartz cell with water to produce a white light continuum as a probe beam. The optical delay line and multiple 10 nm (fwhm) spike filters were also used in these pump−probe measurements with time resolution of ∼300 fs. The sample solutions were placed in a 1 mm quartz flow cell to avoid possible effects of thermooptical distortion and photochemical decomposition.

RESULTS AND DISCUSSION

Linear Photophysical Properties and Photostability of 1−3. The steady-state linear absorption, corrected luminescence, and excitation spectra of **1**−**3** in solvents of different polarity are shown in Figure 2, and the main photophysical and photochemical parameters are summarized in Table 1. Linear 1PA spectra exhibited a weak dependence on solvent polarity and can be assigned to different types of electronic transitions in **1**−**3**. The most intense absorption bands at ≈325 nm (Figure 2a,b, curves 1−3), ≈ 460 nm (curves 2), and ≈440 nm (curves 3) are presumably related to spin-allowed ligand-centered ^{1}(LC) $\pi-\pi^*$ transitions.[3,14] The relatively weak absorption tail for **1** in the spectral range ∼350−550 nm can be assigned to the metal-to-ligand charge-transfer spin-allowed (^{1}MLCT) transitions and extremely weak spin forbidden (^{3}MLCT) transitions at ≥550 nm, respectively.[3,6] The last ones are possibly due to a strong heavy-atom effect on the spin−orbit coupling in Ir(III) complexes.[7,49] It should be mentioned that the majority of ^{1}MLCT transitions in **2** and **3** are spectrally overlapped with the longest-wavelength LC transitions in *dmac* and *minc* ligands. The steady-state luminescence and excitation spectra of **1** were independent of

Table 1. Main Photophysical Parameters of 1−3 in Solvents with Different Polarity Δf[a]: Absorption (λ_{ab}^{max}) and Luminescence (λ_{PL}^{max}) Maxima, Stokes Shifts, Maximum Extinction Coefficients (ε^{max}), PL Quantum Yields Φ_{PL}, lifetimes τ, and photodecomposition quantum yields, Φ_{ph}

N/N	1				2			3			
solvent	TOL	DCM	BTN	ACN	TOL	DCM	BTN	ACN	TOL	DCM	BTN	ACN
λ_{ab}^{max} (nm)	328 ± 1	327 ± 1	326 ± 1	325 ± 1	458 ± 1	462 ± 1	461 ± 1	463 ± 1	440 ± 1	442 ± 1	441 ± 1	442 ± 1
λ_{PL}^{max} (nm)	600 ± 1	605 ± 1	–	613 ± 1	–	578 ± 1	–	625 ± 1	615 ± 1	513 ± 1	–	524 ± 1
Stokes shift (nm) (cm^{-1})	272 ± 2	278 ± 2	–	288 ± 2	–	116 ± 2	–	162 ± 2	175 ± 2	71 ± 2	–	82 ± 2
ε^{max}·10^{-3} (M^{-1}·cm^{-1})	35.8 ± 3	35.1 ± 3	34.7 ± 3	35.1 ± 3	50 ± 5	55 ± 5	57 ± 5	–	50 ± 5	48 ± 5	48 ± 5	45 ± 5
Φ_{PL}[b] (%)	1.3	<1	<1	<1	<1	3.0	<1	<1	<1	<1	<1	<1
τ (ns) (A$_i$)[c]	29[d] ± 1	17[d] ± 1	–	9[d] ± 1	0.8[e]; 0.8 (0.97), 42 (0.03)[f]	1.45[d]	–	0.9 (0.98), 21 (0.02)[g]	0.7 (0.97), 17 (0.03)[h]; 0.8 (0.8), 42 (0.2)[i]	1.45[d]	–	1.0[j]; 1.0 (0.98), 15 (0.02)[d]
Φ_{ph}·10^{5}[k]	0.9	2.4	0.4	1.5	9.4	22	35	–	70	340	400	410

[a]Orientation polarizability $\Delta f = (\varepsilon - 1)/(2\varepsilon + 1) - (n^2 - 1)/(2n^2 + 1)$ (ε and n are the dielectric constant and refractive index of the medium, respectively).[44] [b]$\lambda_{ex} = 373$ nm. [c]Normalized amplitudes of the corresponding lifetime components. [d]$\lambda_{obs} = 600$ nm. [e]$\lambda_{obs} = 525$ nm. [f]$\lambda_{obs} = 630$ nm. [g]$\lambda_{obs} = 640$ nm. [h]$\lambda_{obs} = 550$ nm. [i]$\lambda_{obs} = 620$ nm. [j]$\lambda_{obs} = 540$ nm. [k]$\lambda_{ex} = 405$ nm and laser irradiance ≈ 300 mW/cm^2.

DOI: 10.1021/acs.jpcc.7b06254
J. Phys. Chem. C 2017, 121, 23609−23617

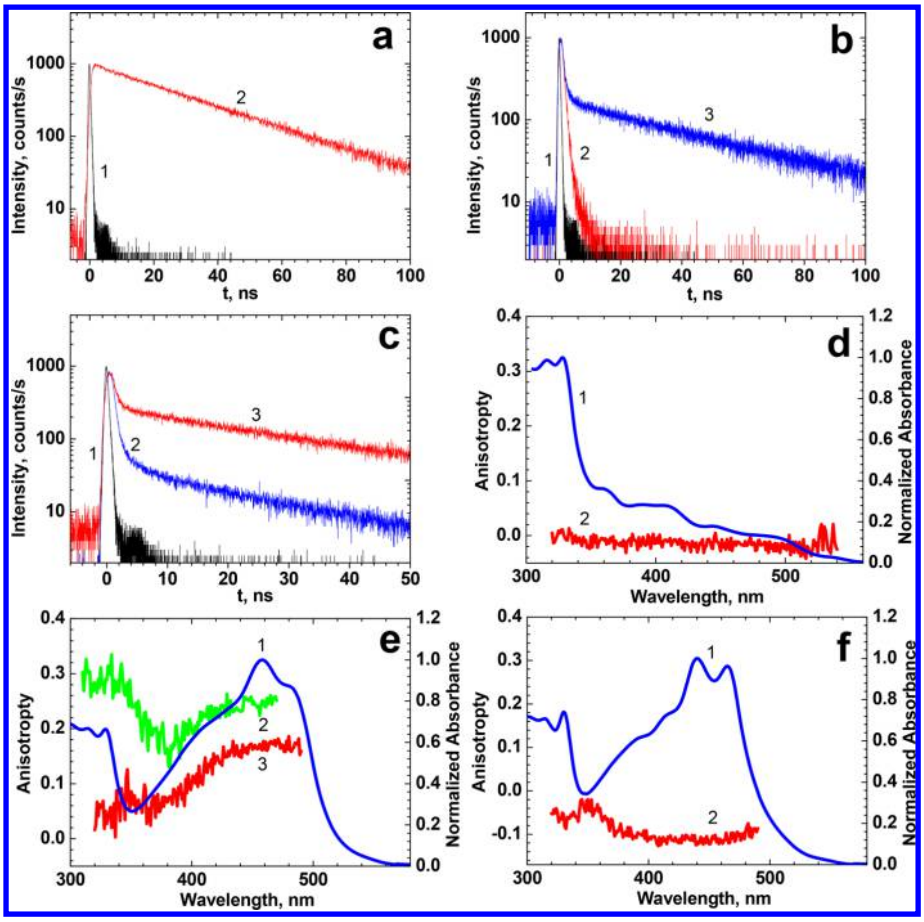

Figure 3. PL decay kinetics of samples **1** (a), **2** (b), and **3** (c) in TOL (curves 1 show the instrument response function). For **1**, curve 2 is for λ_{obs} = 600 nm. For **2**, curve 2 is for λ_{obs} = 525 nm, and curve 3 is for λ_{obs} = 630 nm. For **3**, curve 2 is for λ_{obs} = 550 nm, and curve 3 is for λ_{obs} = 620 nm. Excitation anisotropy spectra in SiO at room temperature of **1** (d), **2** (e), and **3** (f). For **1**, curve 2 is for λ_{obs} = 620 nm; for **2**, curve 2 is for λ_{obs} = 510 nm, curve 3 for 620 nm; and for **3**, curve 2 is for λ_{obs} = 620 nm. The normalized 1PA spectra in panels d–f are labeled 1.

excitation, λ_{ex}, and observed, λ_{obs}, wavelengths, respectively, in contrast to **2** and **3**, where a noticeable dependence of the corrected excitation spectra on λ_{obs} was observed (Figure 2c). This means that chromophore systems of different ligands in the molecular structures of **2** and **3** emit independently and the value of the emission quantum yield, Φ_{PL}, is dependent on λ_{ex} with a corresponding violation of Kasha's rule.[44] All compounds exhibited relatively low values of $\Phi_{PL} \leq 1-3\%$ (see Table 1) with some complicated dependence on solvent polarity Δf. The luminescence decay curves of **1** exhibited a single exponential character in all solvents (see Figure 3a and Table 1) and can be assigned to room-temperature phosphorescence emission. This assumption is based on the low values of the emission quantum yields of **1** (~1%) that give a radiative emission lifetime $\tau_R = \tau/\Phi_{PL} \sim 10^{-5}-10^{-6}$ s which is typical for Ir(III) complex phosphorescence.[17,18] The PL decay curves of **2** and **3** exhibit an obvious double exponential kinetic shape in nonpolar TOL (Figure 3b,c) with significantly different values of lifetime components (Table 1). The short-lived components (~1 ns) can be assigned to fluorescence emission of **2** and **3** in nonpolar media related to spin-allowed radiative transitions from ^{1}LC and/or ^{1}MLCT excited states, while the longer lifetimes correspond to typical room-temperature phosphorescence of Ir(III) complexes from ^{3}MLCT states.[6,50] It should be mentioned that only short nanosecond emission components were observed for **2** and **3** in relatively polar DCM (see Table 1) as evidence of the specific PL lifetime dependence on solvent polarity Δf. In order to explain the nature of the observed spectroscopic peculiarities of complexes **2** and **3** in nonpolar TOL, an electronic model with a double minimum excited-state potential energy surface is proposed, as depicted in Figure 4. According to the model presented, the relative population of these two separate minima of the potential surfaces is a function of the excitation wavelength, λ_{ex}, and therefore results in a noticeable dependence of PL spectra of **2** and **3** on λ_{ex} with corresponding dependences $\Phi_{PL}(\lambda_{ex})$. In contrast, the shape of PL spectra of **1** was independent of λ_{ex}, but the value of its Φ_{PL} exhibits a noticeable decrease in the short wavelength spectral range as evidence of separate ligand absorption without phosphorescence emission.

The steady-state excitation anisotropy spectra of **1**–**3** obtained at room temperature in viscous nonpolar SiO are presented in Figure 3d–f. As follows from these data, the excitation anisotropy is close to zero for the relatively long phosphorescence emission of **1** and reveals some positive values $r(\lambda) \sim 0.15-0.25$ for **2** in the main absorption band due to a fast fluorescence component in the PL spectrum and to small angles (<30–40°) between the absorption and fluorescence emission transition dipoles. In contrast, complex **3** exhibits negative values of anisotropy related to a large angle >54.7° between the absorption and emission dipoles. This can be explained by sufficiently different molecular geometries in the ground and excited electronic states (see Figures S2 and S3). That is also consistent with the different shapes and

DOI: 10.1021/acs.jpcc.7b06254
J. Phys. Chem. C 2017, 121, 23609–23617

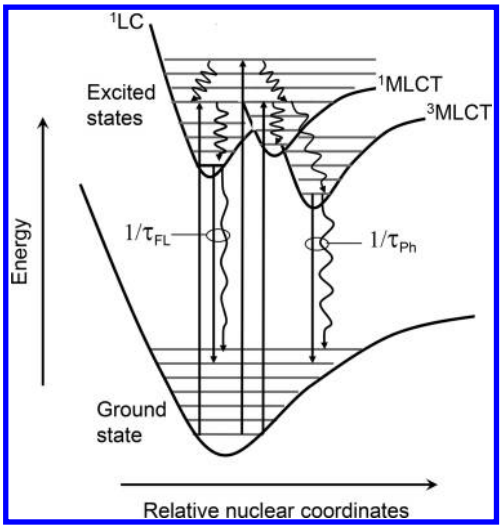

Figure 4. Qualitative model representation of the potential energy diagram of the ground and excited electronic states for Ir(III) complexes **2** and **3** in nonpolar medium. τ_{FL} and τ_{Ph} are the fluorescence and phosphorescence lifetimes, respectively.

spectral positions of the corresponding PL spectra in nonpolar solvents (Figure 2a).

The photochemical stability of the new Ir(III) complexes was investigated quantitatively by the absorption method,[41] and the obtained values of the photodecomposition quantum yields, Φ_{ph}, are presented in Table 1. The observed photochemical stabilities of **1**−**3** are not as high as the best laser dyes ($\Phi_{ph} \sim 10^{-6}$),[51,52] but they acceptable for other practical applications. The highest level of photostability, $\Phi_{ph} \sim 10^{-5}$, was observed for **1** in nonpolar TOL, in contrast to complex **2** and especially for **3**, where the long *dmac* and *minc* ligands probably determine the reduction of the molecular stability under laser irradiation. We carefully considered the question of whether a small impurity (or photodecomposition product) with large fluorescence yield could explain some of the double-exponential photoemission data, e.g., the double-band PL spectrum of **2** in TOL (Figure 2a, curve 2′) might be explained by separate *dmac* ligands and/or possible photochemical products with fluorescence maximum at ∼520 nm. Although such impurities could affect the shape of PL of **2** in TOL, they cannot explain all of the experimental data including transient absorption spectra (see corresponding section below). Given the close spectral shapes of, for example, the free ligands with the [Ir(pbt)2(dmac)] spectrum, spectral measurements cannot completely rule this out. However, transient absorption data strongly support our proposed double-minimum excited-state potential energy surface for **2** and **3**, and all experimental data is in a good agreement with this model's predictions.

2PA Properties of 1−3. The degenerate 2PA spectra of **1**−**3** were obtained by performing open-aperture Z-scans in 1 mm path length quartz cells in TOL solutions with molecular concentrations of 10^{-3}−10^{-4} M and are presented in Figure 5. As follows from these data, the maximum values of 2PA cross sections, $\delta_{2PA} \approx 80$ GM, ≈ 350 GM, and ≈ 270 GM were observed for **1** (a), **2** (b), and **3** (c), respectively. The low efficiency of 2PA in **1** can be assigned to the relatively small values of the $^1S_0 \rightarrow {}^1$MLCT transition dipole moments ($^1S_0$ is the ground electronic state) which are determined by the corresponding small values of extinction coefficients ($\leq 10^4$ M^{-1} cm^{-1}) over the entire visible spectral range. Complexes **2**

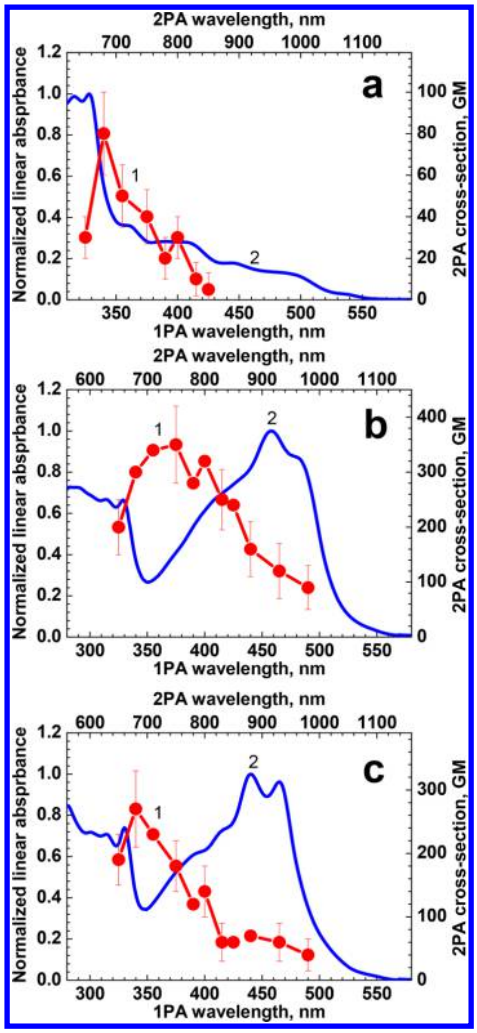

Figure 5. Degenerate 2PA (1) and normalized 1PA (2) spectra of **1** (a), **2** (b), and **3** (c) in TOL.

and **3** exhibit larger values of δ_{2PA}, which are mainly determined by the molecular structures of the *dmac* and *minc* ligands, but the 2PA noticeably decreased in the main linear absorption band. This decrease can be assigned to weak changes in the permanent dipole moments under electronic excitation, $^1S_0 \rightarrow {}^1$LC. The last statement is based on the weak solvatochromic behavior of the LC-related absorption bands and corresponding fluorescence components in the PL spectra of **2** and **3**. It should be mentioned that the restricted solubility of Ir(III) complexes **1**−**3** in TOL did not allow us to obtain 2PA cross sections in the long wavelength range ($\lambda_{ex} > 1000$ nm) by Z-scans.

Transient Absorption Spectroscopy of 1−3. The nature of the fast relaxation processes in the ground and excited electronic states of **1**−**3** were investigated in TOL solution at room temperature by the femtosecond transient absorption pump−probe technique.[45,53] Sample solutions with maximum optical density $D \approx 0.7$−0.8 were pumped at $\lambda_{pu} = 400$ nm ($E_P \approx 2$ μJ), beam waist $\omega_0 \approx 0.4$ mm (HW1/e^2 M), and the value of the induced change in optical density, ΔD, was measured by a weak probe pulse (focused to $\omega_0 \approx 0.1$ mm) as a function of temporal delay, τ_D, between pump and probe pulses. Typical dependences of $\Delta D(\tau_D)$ for different probing wavelengths, λ_{pr}, are shown in Figure 6. As follows from the transient absorption curves, $\Delta D(\tau_D)$, the absolute values of ΔD were positive for the majority of probing wavelengths except for a weak saturable

DOI: 10.1021/acs.jpcc.7b06254
J. Phys. Chem. C 2017, 121, 23609−23617

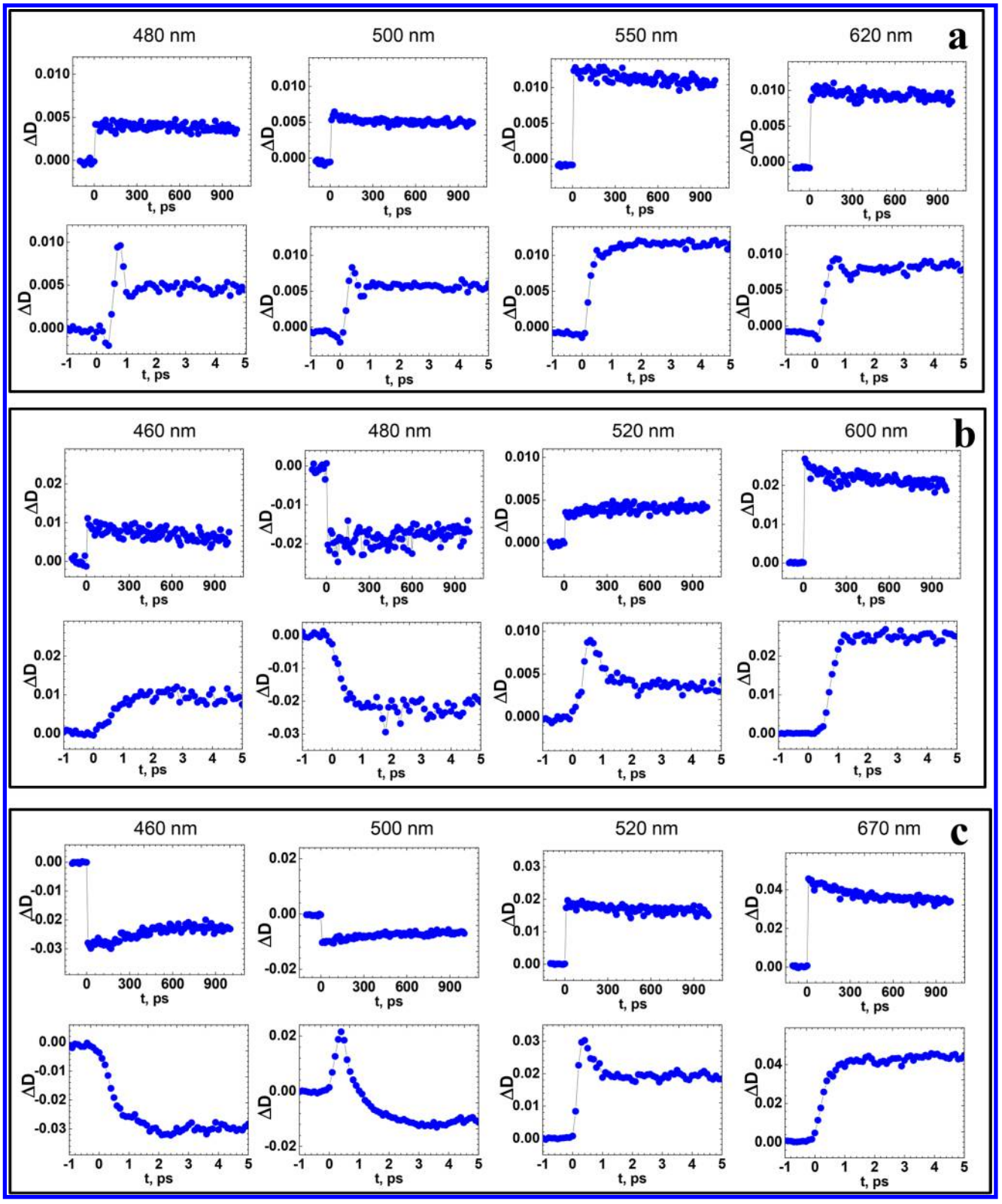

Figure 6. Typical dependences $\Delta D(\tau_D)$ for **1** (a), **2** (b), and **3** (c) in TOL (λ_{pu} = 400 nm): picosecond (top) and femtosecond (bottom) temporal resolution. Corresponding probing wavelengths, λ_{pr}, are indicated on the top.

absorption, SA (negative ΔD) near $\lambda_{pr} \approx 480$ nm for **2** and in the spectral range ~460−500 nm for **3**. The ultrafast relaxation processes in **1** (assumed to be related to ESA) were completed in less than 1 ps after excitation (Figure 6a) without any obvious role of solvatochromic phenomena typically observed on the time scale of 1−10 ps.[45,54] In contrast, complexes **2** and **3** exhibit a slightly longer-lasting fast relaxation (Figure 6b,c) which can be related to possible solvatochromic effects. Taking into account the PL kinetic curves in Figure 3a−c and the relatively small ΔD on the time scale of ~1 ns (Figure 6, top

DOI: 10.1021/acs.jpcc.7b06254
J. Phys. Chem. C 2017, 121, 23609−23617

curves), it can be assumed that the long-lived signals belong to triplet−triplet absorption. This implies extremely fast population (~500 fs) of the triplet electronic states of **1** and ≤2 ps for **2** and **3** in TOL. It should be mentioned that the ultrafast triplet state population of Ir complexes was observed previously for known compounds, such as $Ir(ppy)_3$, $Ir(DBQ)_2(acac)$, and $Ir(MDQ)_2(acac)$ in BTN;[3] $Ir(piq)_3$ in tetrahydrofuran;[26] etc. The time-resolved pump−probe absorption spectra of **1**−**3**, reconstructed from the experimental dependences $\Delta D(\tau_D)$ in a broad spectral range of λ_{pr}, are presented in Figure 7. As follows

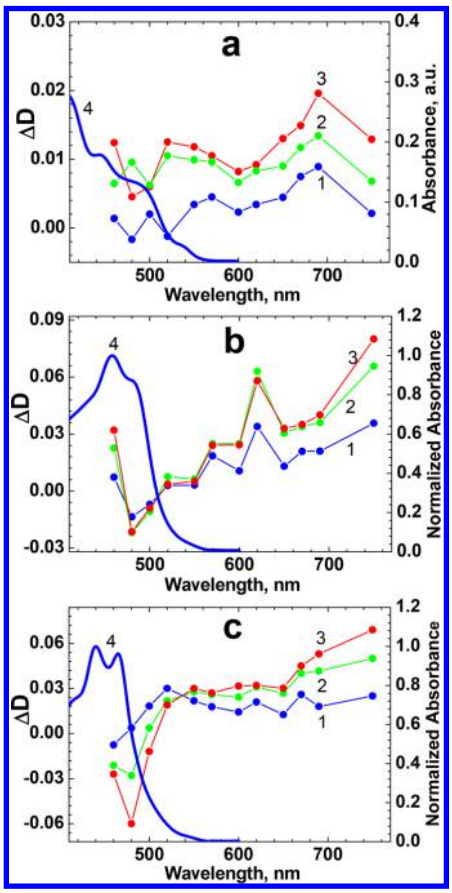

Figure 7. Spectral dependences $\Delta D(\lambda_{pr})$ for samples **1** (a), **2** (b), and **3** (c) in TOL for different time delays τ_D. Curves 1 are for 0.3 ps delay, curves 2 for 0.8 ps, and curves 3 for 5 ps. The linear absorption spectra in TOL are labeled as curve 4.

from these data, the shape of the time-resolved absorption spectra of **1**−**3** in TOL remains nearly the same in the PL spectral range (λ_{pr} > 580 nm) and can be assigned to triplet−triplet absorption. At the same time, the nature of the ultrafast changes in the first 5 ps for λ_{pr} < 580 nm, in addition to triplet−triplet absorption, also includes the effects of SA and ESA between the excited ^{1}LC and/or ^{1}MLCT vibronic states (Figure 6a, λ_{pr} = 480 nm; 6b, 520 nm; 6c, 500 nm, 520 nm).

We mentioned earlier that a strongly fluorescing impurity in the same spectral region as these molecules could be an alternate interpretation of the dual luminescence. However, we have shown that molecules **2** and **3** also exhibit two temporal components of their transient absorption. The concentration of an impurity would have to be so low that the changes in transmission measured in these experiments would be impossible. Additionally, the temporal dependence of the transient absorption closely follows the temporal dependencies observed in the luminescence.

CONCLUSIONS

Three new Ir(III) complexes **1**−**3** bearing β-diketonate ligands were synthesized, and their linear photophysical properties, photostabilities, 2PA spectra, and femtosecond transient absorption kinetics were investigated in a number of organic solvents at room temperature. The nature of the steady-state 1PA spectra of **1**−**3** was determined by the analysis of the multiple electronic transitions involving LC and MLCT vibronic states and their weak dependence on solvent polarity. Complex **1** exhibited PL and excitation spectra almost independent of excitation, λ_{ex}, or observed, λ_{obs}, wavelengths, respectively, and we assign the observed emission spectra to room-temperature phosphorescence. In contrast, complexes **2** and **3** possess dual-band PL emission possessing different lifetimes. We assign these to simultaneous fluorescence (<1 ns) and phosphorescence (>10 ns) processes from ^{1}LC and ^{3}MLCT electronic states, respectively. The excitation spectra of **2** and **3** were noticeably different from the corresponding absorption spectra, and a strong dependence on λ_{obs} was measured along with a similar dependence of their PL spectra on λ_{ex}. These rather unusual spectroscopic observations of **2** and **3** were explained based on the dual-minima excited-state potential surface electronic model that allows nearly independent emission channels in a single molecular structure.

The degenerate 2PA spectra of **1**−**3** were obtained over a broad spectral range by open aperture Z-scans. The maximum cross section values δ_{2PA} ≈ 250−350 GM were shown for **2** and **3** with *dmac* and *minc* ligands, respectively. The investigation of the ultrafast dynamic processes in the ground and excited states of **1**−**3** revealed the characteristic time scale of the triplet level population as <500 fs for complex **1** and ~2 ps for **2** and **3** in nonpolar TOL at room temperature. The linear photophysical and 2PA spectra of these newly synthesized Ir(III) complexes, along with the dual-minimum potential surface of the excited electronic states, can be useful for potential applications of **1**−**3** in the field of organic electronics, nonlinear optics, photodynamic therapy, etc.

ASSOCIATED CONTENT

Supporting Information

The Supporting Information is available free of charge on the ACS Publications website at DOI: 10.1021/acs.jpcc.7b06254.

Synthesis and chemical structures of complexes **1**−**3**, H-1 NMR spectra for **1**−**3**, X-ray crystal structures of **1**−**3**, and experimental details (PDF)

AUTHOR INFORMATION

Corresponding Authors

*E-mail: mbondar@mail.ucf.edu. Tel.: 38-044-525-9968.
*E-mail: ewvs@creol.ucf.edu. Tel.: 1-407-823-6835.

ORCID

Peng Zhao: 0000-0001-6370-4206
Ryan M. O'Donnell: 0000-0002-3565-9783

Notes

The authors declare no competing financial interest.

DOI: 10.1021/acs.jpcc.7b06254
J. Phys. Chem. C 2017, 121, 23609−23617

■ ACKNOWLEDGMENTS

E.V.S., D.J.H., P.Z., and M.V.B. thank the Army Research Laboratory (W911NF-15-2-0090) and the National Science Foundation Grant DMR-1609895 for support. P.Z. thanks the UCF Pre-eminent Postdoctoral Program for funding. M.V.B. thanks the National Academy of Sciences of Ukraine (Grants B-180 and VC/188) and FP7-Marie Curie Actions: ITN "Nano2Fun" GA #607721.

■ REFERENCES

(1) Tsuboi, T.; Huang, W. Recent Advances in Multicolor Emission and Color Tuning of Heteroleptic Iridium Complexes. *Isr. J. Chem.* **2014**, *54*, 885−896.
(2) Bai, W. On a Series of Ir(III) Complexes with Various Numbers of Fluorine Atoms. *J. Lumin.* **2012**, *132*, 2847−2854.
(3) Tang, K.-C.; Liu, K. L.; Chen, I.-C. Rapid Intersystem Crossing in Highly Phosphorescent Iridium Complexes. *Chem. Phys. Lett.* **2004**, *386*, 437−441.
(4) Alam, P.; Kaur, G.; Sarmah, A.; Roy, R. K.; Choudhury, A. R.; Laskar, I. R. Highly Selective Detection of H^+ and OH^- with a Single-Emissive Iridium(III) Complex: A Mild Approach to Conversion of Non-AIEE to AIEE Complex. *Organometallics* **2015**, *34*, 4480−4490.
(5) Fu, J.; Moxey, G. J.; Morshedi, M.; Barlow, A.; Randles, M. D.; Simpson, P. V.; Schwich, T.; Cifuentes, M. P.; Humphrey, M. G. Mixed-Metal Cluster Chemistry. 37. Syntheses, Structural, Spectroscopic, Electrochemical, and Optical Power Limiting Studies of Tetranuclear Molybdenum-Iridium Clusters. *J. Organomet. Chem.* **2016**, *30*, 135.
(6) Liu, D.; Ren, H.; Deng, L.; Zhang, T. Synthesis and Electrophosphorescence of Iridium Complexes Containing Benzothiazole-Based Ligands. *ACS Appl. Mater. Interfaces* **2013**, *5*, 4937−4944.
(7) Cui, L.-S.; Liu, Y.; Liu, X.-Y.; Jiang, Z.-Q.; Liao, L.-S. Design and Synthesis of Pyrimidine-Based Iridium(III) Complexes with Horizontal Orientation for Orange and White Phosphorescent OLEDs. *ACS Appl. Mater. Interfaces* **2015**, *7*, 11007−11014.
(8) Yang, H.; Li, L.; Wan, L.; Zhou, Z.; Yang, S. Synthesis of Water Soluble Peg-Functionalized Iridium Complex Via Click Chemistry and Application for Cellular Bioimaging. *Inorg. Chem. Commun.* **2010**, *13*, 1387−1390.
(9) Ma, D.-L.; Zhong, H.-J.; Fu, W.-C.; Chan, D. S.-H.; Kwan, H.-Y.; Fong, W.-F.; Chung, L.-H.; Wong, C.-Y.; Leung, C.-H. Phosphorescent Imaging of Living Cells Using a Cyclometalated Iridium(III) Complex. *PLoS One* **2013**, *8*, e55751.
(10) Martí, A. A. Metal Complexes and Time-Resolved Photoluminescence Spectroscopy for Sensing Applications. *J. Photochem. Photobiol., A* **2015**, *307*−*308*, 35−47.
(11) Xu, W.-J.; Liu, S.-J.; Zhao, X.; Zhao, N.; Liu, Z.-Q.; Xu, H.; Liang, H.; Zhao, Q.; Yu, X.-Q.; Huang, W. Synthesis, One- and Two-Photon Photophysical and Excited-State Properties, and Sensing Application of a New Phosphorescent Dinuclear Cationic Iridium(III) Complex. *Chem. - Eur. J.* **2013**, *19*, 621−629.
(12) Colombo, A.; Dragonetti, C.; Roberto, D.; Valore, A.; Ferrante, C.; Fortunati, I.; Picone, A. L.; Todescato, F.; Williams, J. A. G. Two-Photon Absorption Properties and $^1O_2$ Generation Ability of Ir Complexes: An Unexpected Large Cross Section of $[Ir(CO)_2Cl$-(4-(*Para*-Di-*N*-Butylaminostyryl)Pyridine)]. *Dalton Trans.* **2015**, *44*, 15712−15720.
(13) Adachi, C.; Baldo, M. A.; Thompson, M. E.; Forrest, S. R. Nearly 100% Internal Phosphorescence Efficiency in an Organic Light Emitting Device. *J. Appl. Phys.* **2001**, *90*, 5048−5051.
(14) Hajra, T.; Bera, J. K.; Chandrasekhar, V. Cyclometalated Ir(III) Complexes Containing Pyrazole/Pyrazine Carboxylate Ligands. *Aust. J. Chem.* **2011**, *64*, 561−566.
(15) Lamansky, S.; Djurovich, P.; Murphy, D.; Abdel-Razzaq, F.; Kwong, R.; Tsyba, I.; Bortz, M.; Mui, B.; Bau, R.; Thompson, M. E. Synthesis and Characterization of Phosphorescent Cyclometalated Iridium Complexes. *Inorg. Chem.* **2001**, *40*, 1704−1711.
(16) Chew, S.; Lee, C. S.; Lee, S.-T.; Wang, P.; He, J.; Li, W.; Pan, J.; Zhang, X.; Kwong, H. Photoluminescence and Electroluminescence of a New Blue-Emitting Homoleptic Iridium Complex. *Appl. Phys. Lett.* **2006**, *88*, 093510.
(17) Tsuboi, T.; Aljaroudi, N. Relaxation Processes in the Triplet State T1 of Organic Ir-Compound $Btp_2Ir(acac)$ Doped in PC and CBP Fluorescent Materials. *J. Lumin.* **2006**, *119*−*120*, 127−131.
(18) Lamansky, S.; Djurovich, P.; Murphy, D.; Abdel-Razzaq, F.; Lee, H.-E.; Adachi, C.; Burrows, P. E.; Forrest, S. R.; Thompson, M. E. Highly Phosphorescent Bis-Cyclometalated Iridium Complexes: Synthesis, Photophysical Characterization, and Use in Organic Light Emitting Diodes. *J. Am. Chem. Soc.* **2001**, *123*, 4304−4312.
(19) Beeby, A.; Bettington, S.; Samuel, I. D. W.; Wang, Z. Tuning the Emission of Cyclometalated Iridium Complexes by Simple Ligand Modification. *J. Mater. Chem.* **2003**, *13*, 80−83.
(20) Bezzubov, S. I.; Kiselev, Y. M.; Churakov, A. V.; Kozyukhin, S. A.; Sadovnikov, A. A.; Grinberg, V. A.; Emets, V. V.; Doljenko, V. D. Iridium(III) 2-Phenylbenzimidazole Complexes: Synthesis, Structure, Optical Properties, and Applications in Dye-Sensitized Solar Cells. *Eur. J. Inorg. Chem.* **2016**, *2016*, 347−354.
(21) Lyu, Y.-Y.; Byun, Y.; Kwon, O.; Han, E.; Jeon, W. S.; Das, R. R.; Char, K. Substituent Effect on the Luminescent Properties of a Series of Deep Blue Emitting Mixed Ligand Ir(III) Complexes. *J. Phys. Chem. B* **2006**, *110*, 10303−10314.
(22) Tian, N.; Thiessen, A.; Schiewek, R.; Schmitz, O. J.; Hertel, D.; Meerholz, K.; Holder, E. Efficient Synthesis of Carbazolyl- and Thienyl-Substituted *B*-Diketonates and Properties of Their Red- and Green-Light-Emitting Ir(III) Complexes. *J. Org. Chem.* **2009**, *74*, 2718−2725.
(23) Aoki, S.; Matsuo, Y.; Ogura, S.; Ohwada, H.; Hisamatsu, Y.; Moromizato, S.; Shiro, M.; Kitamura, M. Regioselective Aromatic Substitution Reactions of Cyclometalated Ir(III) Complexes: Synthesis and Photochemical Properties of Substituted Ir(III) Complexes That Exhibit Blue, Green, and Red Color Luminescence Emission. *Inorg. Chem.* **2011**, *50*, 806−818.
(24) Duan, H.-S.; Chou, P.-T.; Hsu, C.-C.; Hung, J.-Y.; Chi, Y. Photophysics of Heteroleptic Iridium(III) Complexes of Current Interest; a Closer Look on Relaxation Dynamics. *Inorg. Chem.* **2009**, *48*, 6501−6508.
(25) Spaenig, F.; Olivier, J.-H.; Prusakova, V.; Retailleau, P.; Ziessel, R.; Castellano, F. N. Excited-State Properties of Heteroleptic Iridium(III) Complexes Bearing Aromatic Hydrocarbons with Extended Cores. *Inorg. Chem.* **2011**, *50*, 10859−10871.
(26) Hedley, G. J.; Ruseckas, A.; Samuel, I. D. W. Ultrafast Intersystem Crossing in a Red Phosphorescent Iridium Complex. *J. Phys. Chem. A* **2009**, *113*, 2−4.
(27) Pomarico, E.; Silatani, M.; Messina, F.; Braem, O.; Cannizzo, A.; Barranoff, E.; Klein, J. H.; Lambert, C.; Chergui, M. Dual Luminescence, Interligand Decay, and Nonradiative Electronic Relaxation of Cyclometalated Iridium Complexes in Solution. *J. Phys. Chem. C* **2016**, *120*, 16459−16469.
(28) Wang, X.-Y.; Prabhu, R. N.; Schmehl, R. H.; Weck, M. Polymer-Based Tris(2-Phenylpyridine)Iridium Complexes. *Macromolecules* **2006**, *39*, 3140−3146.
(29) Djurovich, P. I.; Watts, R. J. Time-Resolved Transient Difference Absorption Spectra of Iridium-Silicon Bonded Complexes: Evidence for a Solvated Intermediate Formed Via Iridium-Silicon Bond Cleavage. *J. Phys. Chem.* **1994**, *98*, 396−397.
(30) Winkler, J. R.; Marshall, J. L.; Netzel, T. L.; Gray, H. B. Picosecond Spectroscopic Studies of (d^8-d^8) Binuclear Rhodium and Iridium Complexes: A Comparison of $^1b_2$ and $^3b_2$ Reactivity in Bis(1,5-Cyclooctadiene)Bis(M-Pyrazolyl)Diiridium(I). *J. Am. Chem. Soc.* **1986**, *108*, 2263−2266.
(31) Sun, W.; Pei, C.; Lu, T.; Cui, P.; Li, Z.; McCleese, C.; Fang, Y.; Kilina, S.; Song, Y.; Burda, C. Reverse Saturable Absorbing Cationic Iridium(III) Complexes Bearing the 2-(2-Quinolinyl)Quinoxaline Ligand: Effects of Different Cyclometalating Ligands on Linear and Nonlinear Absorption. *J. Mater. Chem. C* **2016**, *4*, 5059−5072.

DOI: 10.1021/acs.jpcc.7b06254
J. Phys. Chem. C 2017, 121, 23609−23617

(32) Kim, K.-Y.; Farley, R. T.; Schanze, K. S. An Iridium(III) Complex That Exhibits Dual Mechanism Nonlinear Absorption. *J. Phys. Chem. B* **2006**, *110*, 17302−17304.
(33) Wu, S.-H.; Ling, J.-W.; Lai, S.-H.; Huang, M.-J.; Cheng, C. H.; Chen, I.-C. Dynamics of the Excited States of $[Ir(ppy)_2bpy]^+$ with Triple Phosphorescence. *J. Phys. Chem. A* **2010**, *114*, 10339−10344.
(34) Tanaka, I.; Tabata, Y.; Tokito, S. Comparison of Phosphorescence Properties of Green-Emitting $Ir(ppy)_3$ and Red-Emitting $Btp_2Ir(acac)$. *Jpn. J. Appl. Phys.* **2004**, *43*, L1601−L1603.
(35) Ragni, R.; Plummer, E. A.; Brunner, K.; Hofstraat, J. W.; Babudri, F.; Farinola, G. M.; Naso, F.; De Cola, L. Blue Emitting Iridium Complexes: Synthesis, Photophysics and Phosphorescent Devices. *J. Mater. Chem.* **2006**, *16*, 1161−1170.
(36) Li, Y.; Dandu, N.; Liu, R.; Hu, L.; Kilina, S.; Sun, W. Nonlinear Absorbing Cationic Iridium(III) Complexes Bearing Benzothiazolylfluorene Motif on the Bipyridine (N∧N) Ligand: Synthesis, Photophysics and Reverse Saturable Absorption. *ACS Appl. Mater. Interfaces* **2013**, *5*, 6556−6570.
(37) Ho, M.-L.; Lin, M.-H.; Chen, Y.-T.; Sheu, H.-S. Iridium(III) Complexes in Discs for Two-Photon Excitation Applications. *Chem. Phys. Lett.* **2011**, *509*, 162−168.
(38) Kim, O.-H.; Ha, S.-W.; Kim, J. I.; Lee, J.-K. Excellent Photostability of Phosphorescent Nanoparticles and Their Application as a Color Converter in Light Emitting Diodes. *ACS Nano* **2010**, *4*, 3397−3405.
(39) Jin, C.; Liu, J.; Chen, Y.; Guan, R.; Ouyang, C.; Zhu, Y.; Ji, L.; Chao, H. Cyclometalated Iridium(III) Complexes as Aie Phosphorescent Probes for Real-Time Monitoring of Mitophagy in Living Cells. *Sci. Rep.* **2016**, *6*, 22039.
(40) Donato, L.; Abel, P.; Zysman-Colman, E. Cationic Iridium(III) Complexes Bearing a Bis(Triazole) Ancillary Ligand. *Dalton Trans.* **2013**, *42*, 8402−8412.
(41) Corredor, C. C.; Belfield, K. D.; Bondar, M. V.; Przhonska, O. V.; Yao, S. One- and Two-Photon Photochemical Stability of Linear and Branched Fluorene Derivatives. *J. Photochem. Photobiol., A* **2006**, *184* (1−2), 105−112.
(42) Baranoff, E.; Curchod, B. F. E.; Frey, J.; Scopelliti, R.; Kessler, F.; Tavernelli, I.; Rothlisberger, U.; Grätzel, M.; Nazeeruddin, M. K. Acid-Induced Degradation of Phosphorescent Dopants for OLEDs and Its Application to the Synthesis of Tris-Heteroleptic Iridium(III) Bis-Cyclometalated Complexes. *Inorg. Chem.* **2012**, *51*, 215−224.
(43) Frey, J.; Curchod, B. F. E.; Scopelliti, R.; Tavernelli, I.; Rothlisberger, U.; Nazeeruddin, M. K.; Baranoff, E. Structure−Property Relationships Based on Hammett Constants in Cyclometalated Iridium(III) Complexes: Their Application to the Design of a Fluorine-Free Firpic-Like Emitter. *Dalton Trans.* **2014**, *43*, 5667−5679.
(44) Lakowicz, J. R. *Principles of Fluorescence Spectroscopy*.; Kluwer: New York, 1999.
(45) Liu, T.; Bondar, M. V.; Belfield, K. D.; Anderson, D.; Masunov, A. E.; Hagan, D. J.; Van Stryland, E. W. Linear Photophysics and Femtosecond Nonlinear Spectroscopy of a Star-Shaped Squaraine Derivative with Efficient Two-Photon Absorption. *J. Phys. Chem. C* **2016**, *120*, 11099−11110.
(46) Belfield, K. D.; Bondar, M. V.; Morales, A. R.; Yue, X.; Luchita, G.; Przhonska, O. V. Transient Excited-State Absorption and Gain Spectroscopy of a Two-Photon Absorbing Probe with Efficient Superfluorescent Properties. *J. Phys. Chem. C* **2012**, *116*, 11261−11271.
(47) Sheik-Bahae, M.; Said, A. A.; Wei, T. H.; Hagan, D. J.; Van Stryland, E. W. Sensitive Measurement of Optical Nonlinearities Using a Single Beam. *IEEE J. Quantum Electron.* **1990**, *26* (4), 760−769.
(48) Belfield, K. D.; Bondar, M. V.; Haniff, H. S.; Mikhailov, I. A.; Luchita, G.; Przhonska, O. V. Superfluorescent Squaraine with Efficient Two-Photon Absorption and High Photostability. *ChemPhysChem* **2013**, *14*, 3532−3542.
(49) Holzer, W.; Penzkofer, A.; Tsuboi, T. Absorption and Emission Spectroscopic Characterization of $Ir(ppy)_3$. *Chem. Phys.* **2005**, *308*, 93−102.
(50) Yoshikawa, N.; Matsumura-Inoue, T. Electrochemical and Phosphorescent Properties of New Mixed-Ligand Ir(III) Complexes Coordinated with Both Terpyridine and Various Bipyridine Derivatives. *Anal. Sci.* **2003**, *19*, 761−765.
(51) Rosenthal, I. Photochemical Stability of Rhodamine 6G in Solution. *Opt. Commun.* **1978**, *24* (2), 164−166.
(52) El-Daly, S. A.; El-Azim, S. A.; Elmekawey, F. M.; Elbaradei, B. Y.; Shama, S. A.; Asiri, A. M. Photophysical Parameters, Excitation Energy Transfer, and Photoreactivity of 1,4-Bis(5-Phenyl-2-Oxazolyl)-Benzene (POPOP) Laser Dye. *Int. J. Photoenergy* **2012**, *2012*, 458126.
(53) Lepkowicz, R. S.; Przhonska, O. V.; Hales, J. M.; Hagan, D. J.; Van Stryland, E. W.; Bondar, M. V.; Slominsky, Y. L.; Kachkovski, A. D. Excited-State Absorption Dynamics in Polymethine Dyes Detected by Polarization-Resolved Pump-Probe Measurements. *Chem. Phys.* **2003**, *286* (2−3), 277−291.
(54) Yue, X.; Armijo, Z.; King, K.; Bondar, M. V.; Morales, A. R.; Frazer, A.; Mikhailov, I. A.; Przhonska, O. V.; Belfield, K. D. Steady-State and Femtosecond Transient Absorption Spectroscopy of New Two-Photon Absorbing Fluorene-Containing Quinolizinium Cation Membrane Probes. *ACS Appl. Mater. Interfaces* **2015**, *7*, 2833−2846.

DOI: 10.1021/acs.jpcc.7b06254
J. Phys. Chem. C 2017, 121, 23609−23617